NACA

RESEARCH MEMORANDUM

LOW-SPEED INVESTIGATION OF THE EFFECTS OF WING DIHEDRAL ANGLE AND FIN LENGTH ON THE STATIC STABILITY CHARACTERISTICS OF A MODEL HAVING AN 82° DELTA WING

By Kenneth P. Spreemann

Langley Aeronautical Laboratory
Langley Field, Va.

NATIONAL ADVISORY COMMITTEE
FOR AERONAUTICS

WASHINGTON

April 2, 1956

NATIONAL ADVISORY COMMITTEE FOR AERONAUTICS

RESEARCH MEMORANDUM

LOW-SPEED INVESTIGATION OF THE EFFECTS OF WING DIHEDRAL ANGLE AND FIN LENGTH ON THE STATIC STABILITY CHARACTERISTICS OF A MODEL HAVING AN 82° DELTA WING

By Kenneth P. Spreemann

SUMMARY

An investigation was conducted in the Langley 300 MPH 7- by 10-foot tunnel at dynamic pressures of 40 and 60 pounds per square foot and corresponding Reynolds numbers of 6.09×10^6 and 7.42×10^6, based on the mean aerodynamic chord, to determine the effects of changes in wing dihedral angle and length and position of fins on the static stability characteristics of an 82° delta-wing—body configuration. Wing dihedral angles of 0° and ±30° and three fins of different lengths mounted above and below the fuselage were investigated.

Changes in the wing dihedral from 0° to ±30° reduced the lift-curve slopes of the model. These reductions in the lift-curve slopes were reflected in the drag polar, so that appreciably higher drag at a given lift coefficient was evident for the wings with dihedral. All three complete-model configurations were longitudinally stable through most of the angle-of-attack range.

A medium length fin that extended from the point about which the moments were measured (about 58 percent of the fuselage length) to approximately 95 percent of the fuselage length, provided the greatest directional stability. All configurations with fins on top of the fuselage had positive dihedral effect through the lift range; whereas, for the configuration with the fin on the bottom, negative dihedral effect occurred for all fin lengths in the lower lift range. Moreover, the configuration having the large fin below the body, in combination with the 30° dihedral wing, provided increasing values of negative dihedral effect with increasing angle of attack.

[redacted]

INTRODUCTION

An airplane configuration employing highly swept delta wings in combination with a high-fineness-ratio body has been considered as a possible arrangement for flight at high supersonic speeds.

A low-speed investigation of one variation of a model that might meet these requirements is reported in reference 1. The present investigation also was conducted at low speed; however, the model configuration is somewhat different from that of reference 1 and some additional variables are considered. The present wing was triangular in plan form and had a leading-edge sweep angle of 82° and an aspect ratio of 0.56. Wing dihedral angles of 0° and ±30° and fins of three different lengths mounted either above or below the fuselage were investigated. The investigation was conducted in the Langley 300 MPH 7- by 10-foot tunnel at dynamic pressures of 40 and 60 pounds per square foot and corresponding Reynolds numbers of 6.09×10^6 and 7.42×10^6, based on the mean aerodynamic chord.

COEFFICIENTS AND SYMBOLS

The stability and body axes systems used for presentation of the data, together with an indication of the positive directions of forces, moments, and angles, are presented in figure 1. All moments are referred to the 44.2-percent-chord point of the mean aerodynamic chord which is located at 58.2 percent of the body length.

C_A axial-force coefficient, F_A/qS

C_D drag coefficient, F_D/qS

C_L lift coefficient, F_L/qS

$C_{l,s}$ rolling-moment coefficient referred to stability axes, M_{x_s}/qSb

C_l rolling-moment coefficient referred to body axes, M_X/qSb

C_m pitching-moment coefficient, $M_Y/qS\bar{c}$

C_N normal-force coefficient, F_N/qS

$C_{n,s}$	yawing-moment coefficient referred to stability axes, M_{Z_s}/qSb
C_n	yawing-moment coefficient referred to body axes, M_Z/qSb
C_Y	side-force coefficient, F_Y/qS
F_A	axial force, positive along -X-axis, lb
F_D	drag force, positive along $-X_s$-axis, lb
F_L	lift force, positive along $-Z_s$-axis, lb
F_N	normal force, positive along -Z-axis, lb
F_Y	side force, positive along Y_s- or Y-axis, lb
M_{X_s}	rolling moment about the X_s-axis, positive clockwise looking forward, ft-lb
M_X	rolling moment about the X-axis, positive clockwise looking forward, ft-lb
M_Y	pitching moment about the Y_s- or Y-axis, positive moment raises nose, ft-lb
M_{Z_s}	yawing moment about Z_s-axis, positive moment rotates nose to right looking forward, ft-lb
M_Z	yawing moment about Z-axis, positive moment rotates nose to right looking forward, ft-lb
X_s,Y_s,Z_s	axes in stability system (fig. 1)
X,Y,Z	axes in body system (fig. 1)
S	wing area, sq ft (includes area within fuselage)
b	wing span, 2.28 ft on model
$\bar{c}$	mean aerodynamic chord of wing, $\frac{2}{S}\int_0^{b/2} c^2\,dy$, 5.25 ft on model
c	local wing chord, parallel to plane of symmetry, ft

c_i chord of largest fin at intersection of fuselage

q dynamic pressure, lb/sq ft

V free-stream velocity, ft/sec

α angle of attack, deg

β angle of sideslip, deg

Λ leading-edge sweep angle, deg

Γ dihedral angle, deg

$$\left(C_{l,s}\right)_\beta = \frac{\partial C_{l,s}}{\partial \beta} \text{ per deg}$$

$$C_{l_\beta} = \frac{\partial C_l}{\partial \beta} \text{ per deg}$$

$$\left(C_{n,s}\right)_\beta = \frac{\partial C_{n,s}}{\partial \beta} \text{ per deg}$$

$$C_{n_\beta} = \frac{\partial C_n}{\partial \beta} \text{ per deg}$$

$$C_{Y_\beta} = \frac{\partial C_Y}{\partial \beta} \text{ per deg}$$

MODEL AND APPARATUS

The model was tested on a single-support strut in the Langley 300 MPH 7- by 10-foot tunnel.

The model consisted of an 82° swept triangular wing and vertical fins of three different lengths attached to a cylindrical body of fineness ratio 10.74 with an ogival nose as shown in figure 2. The wings and fins were made of 1/2-inch plywood with beveled trailing edges and rounded leading edges. Three dihedral angles (0° and ±30°) were employed on the model. Three fins of different lengths above and below the fuselage were tested with the 0° dihedral wing as shown in figure 2.

[redacted]

TESTS AND CORRECTIONS

The tests in sideslip were made at dynamic pressures of 40 pounds per square foot; whereas all other tests were made at 60 pounds per square foot. The corresponding airspeeds were approximately 125 and 154 miles per hour, and the Reynolds numbers for these airspeeds, based on the mean aerodynamic chord, were 6.09×10^6 and 7.42×10^6, respectively. Forces and moments were measured through an angle-of-attack range of approximately -4° to 35° and a sideslip range of -20° to $+20^\circ$. The lateral-parameter tests were made at $\pm 5^\circ$ sideslip through an angle-of-attack range of -4° to 35°.

Three fins lengths in combination with the 0° dihedral wing were tested above and below the fuselage. Tests were also made with 30° negative dihedral and the largest fin above the fuselage, and with 30° dihedral and the largest fin below the fuselage.

Blockage corrections were determined by the method of reference 2 and were applied to the dynamic pressures. Jet-boundary corrections, applied to the angle of attack and drag, were calculated by the method of reference 3. A buoyancy correction was applied to the data to account for a longitudinal static pressure gradient in the tunnel.

RESULTS AND DISCUSSION

The data are presented in figures 3 to 8. The lateral-stability parameters presented in figures 6 to 8 were evaluated from angle-of-attack tests at $\beta = \pm 5^\circ$.

Longitudinal Stability Characteristics

Lift, drag, and pitching-moment coefficients about the stability axes, and normal and axial forces about the body axes for the model with 0° and $\pm 30^\circ$ dihedral and the fuselage alone are presented in figure 3. From figure 3(a) it can be observed that $\partial C_L/\partial \alpha$ is reduced about 20 to 30 percent above an angle of attack of 8° when going from a dihedral angle of 0° to $\pm 30^\circ$. These changes in $\partial C_L/\partial \alpha$ are further emphasized in the data of figure 3(a) concluded which show considerably lower drag due to lift for the 0° Γ wing. This decrease in drag is approximately proportional to the increase in $\partial C_L/\partial \alpha$.

All three wing arrangements generally provided stable pitching-moment characteristics, except at very high angles of attack (fig. 3(a)

concluded). The large differences in pitching-moment coefficients at zero angle of attack for the different configurations may be caused largely by strut-tare effects - also, deviations from symmetry for the different models may have contributed to the results shown in figure 3.

The normal- and axial-force coefficients (body-axes data), presented in figure 3(b), bear the expected relation to the previous stability-axes results.

Lateral-Stability Characteristics

The lateral-stability data are presented in figures 4 to 8. Lateral coefficients of the 0° dihedral wing shown in figure 4 indicate small amounts of directional instability about the stability axes at 0.2° and 16.4° angles of attack in the medium β range; whereas at 24.6° angle of attack the model was stable, although nonlinearities existed at all angles of attack. Figure 4(b) shows that with respect to the body axes, considerable directional instability existed at angles of attack of 16.4° and 24.6° throughout the β range. Positive dihedral effect (negative C_{l_β}) was indicated regardless of which axes system was considered.

With a negative dihedral angle of 30°, the model was directionally stable about the stability axes (fig. 5(a)). However, with respect to the body axes (fig. 5(b)) the model was about neutrally stable at 16.4° but became quite unstable at 24.6°. Since the model supposedly was laterally symmetrical, the asymmetry in the yawing moments is unexplainable exept for the possibility that the fin, which was attached to the fuselage by means of three sets of angle brackets, may have been asymmetrically deflected under load.

In general, the variations of lateral-stability parameters with α and C_L for all configurations were nonlinear, especially in the high angle-of-attack and lift range. The lateral-stability parameters of the 0° Γ model with three different fin lengths above the fuselage and of the -30° Γ model with the large fin are presented in figure 6. Of the three fins investigated with the wing at 0° Γ, the medium-length fin appeared to provide the most desirable directional-stability characteristics. The directional instability of the model with the longest fin may be attributed to the destabilizing contribution of the portion of the fin ahead of the balance center, which, when combined with the unstable moment of the fuselage alone, was sufficient to nullify the stabilizing moment of the aft portion of the fin, figures 6(a) and 8(a). The -30° Γ wing contributed sufficient directional stability to make the model stable about the stability axes, although some instability with respect to the body axes was indicated. All the configurations of figure 6 (fins on top of fuselage) possessed positive dihedral effect.

[redacted]

The absolute magnitude of C_{Y_β} was increased by the negative dihedral wing (fig. 6(a)), which could be expected as a result of the increased side area of the model when projected in the vertical plane.

The lateral stability parameters of the 0° Γ model with three fins of different lengths below the fuselage and, in addition, a 30° Γ model with the largest fin are presented in figure 7. The largest fin in combination with the 0° Γ wing resulted in a directionally unstable configuration throughout the α and C_L range. The two smaller fins provided marginal stability with respect to either axes system through most ranges of α and C_L. (See figs. 7(a) and 7(b).) With 30° Γ and the large fin on the bottom, the model was stable about the stability axes below 32° angle of attack. With respect to the body axes, the 30° Γ configuration gave large increases in directional stability with α and C_L. For all three fin sizes on the bottom of the fuselage, the model with the 0° Γ wing had negative dihedral effect at low angles of attack and positive dihedral effect at high angles of attack; whereas for the 30° Γ configuration the negative dihedral effect increased in magnitude with angle of attack. The derivative C_{Y_β} was very large, particularly at high angles of attack, for the 30° Γ configuration.

Lateral stability derivatives obtained from breakdown tests of the 0° Γ configuration are presented in figure 8. Above an angle of attack of about 10° the directional instability of wing-fuselage combination was greater than that of the fuselage alone. The wing contributed increasing positive effective dihedral with increasing angle of attack on the stability axes system and a somewhat similar effect, although smaller, with respect to the body axes. The fin contributed a reasonably constant increment of positive effective dihedral through the angle-of-attack range for the stability axes system, however for the body axes the contribution increased above about 15° angle of attack. The displacement of C_{l_β} from 0 for the fuselage alone (fig. 8) is not clearly understood. This discrepancy may result in part to some asymmetry either in the model-support fairing or in the tunnel air flow. In addition, the accuracy level of the measurements would be expected to cause some small errors.

CONCLUSIONS

An investigation at low speeds of the static stability characteristics of an 82° delta wing with dihedral angles of 0° and ±30° in combination with fins of different lengths and a high-fineness-ratio body of revolution indicates the following conclusions:

[redacted]

1. Changes in wing dihedral angle from 0° to ±30° reduced the lift-curve slopes of the model. These reductions were reflected in the drag polar so that appreciably higher drag at a given lift coefficient was evident for the wings with dihedral.

2. All three complete-model configurations were longitudinally stable through most of the angle-of-attack and lift range.

3. A medium-length fin that extended from the point about which the moments were measured (about 58 percent of the fuselage length) to approximately 95 percent of the fuselage length, provided the greatest directional stability.

4. All configurations with fins on top of the fuselage had positive effective dihedral throughout the lift range, whereas, for the configuration with the fin on the bottom, negative dihedral effect occurred for all fin lengths in the lower lift range. Moreover, the configuration having the large fin below the fuselage, in combination with the 30° dihedral wing provided increasing values of negative dihedral effect with increasing angle of attack.

Langley Aeronautical Laboratory,
National Advisory Committee for Aeronautics,
Langley Field, Va., December 12, 1955.

REFERENCES

1. Delany, Noel K.: Exploratory Investigation of the Low-Speed Static Stability of a Configuration Employing Three Identical Triangular Wing Panels and a Body of Equal Length. NACA RM A55C28, 1955.

2. Herriot, John G.: Blockage Corrections for Three-Dimensional-Flow Closed-Throat Wind Tunnels, With Consideration of the Effect of Compressibility. NACA Rep. 995, 1950. (Supersedes NACA RM A7B28.)

3. Gillis, Clarence L., Polhamus, Edward C., and Gray, Joseph L., Jr.: Charts for Determining Jet-Boundary Corrections for Complete Models in 7- by 10-Foot Closed Rectangular Wind Tunnels. NACA WR L-123, 1945. (Formerly NACA ARR L5G31.)

[redacted]

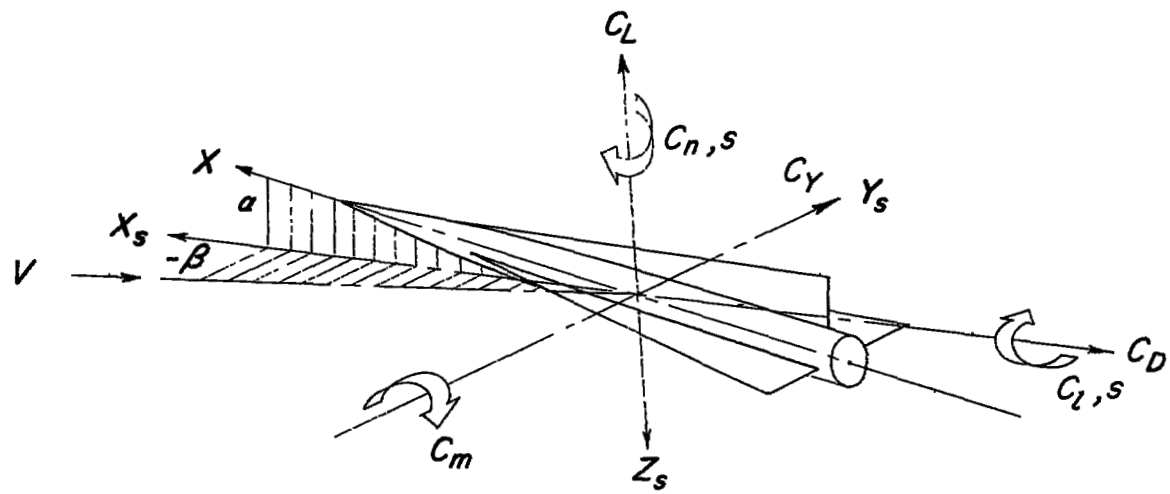

(a) Stability axes.

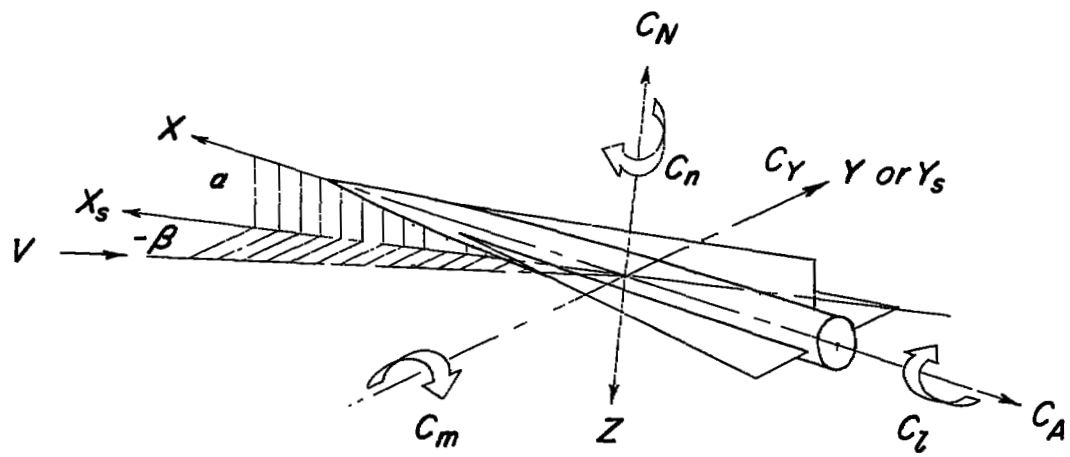

(b) Body axes.

Figure 1.- Systems of axes used. Positive directions of forces and moments are indicated by arrows.

[redacted]

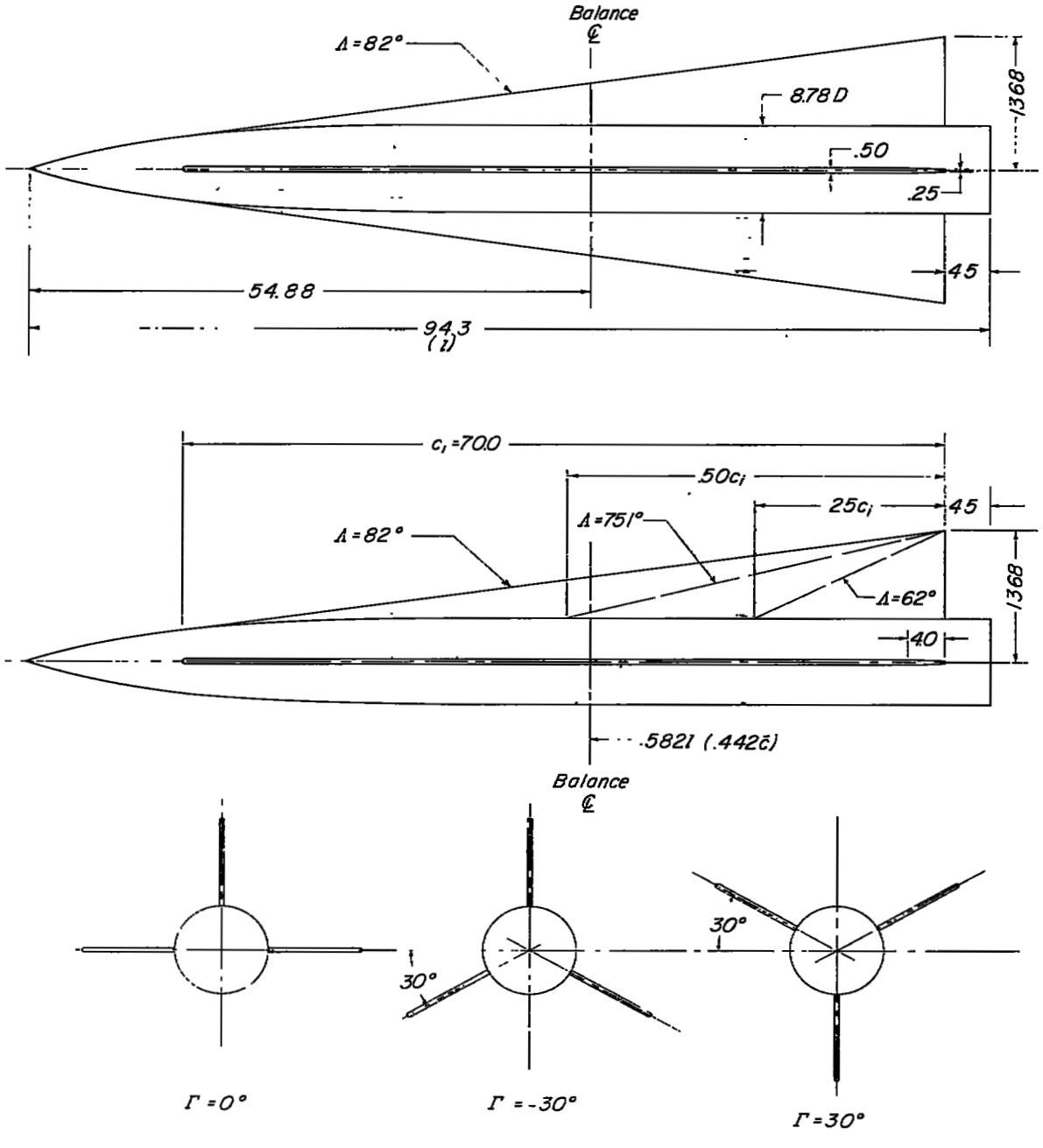

Figure 2.- Test model showing details of various configurations employed. All dimensions are in inches.

[redacted]

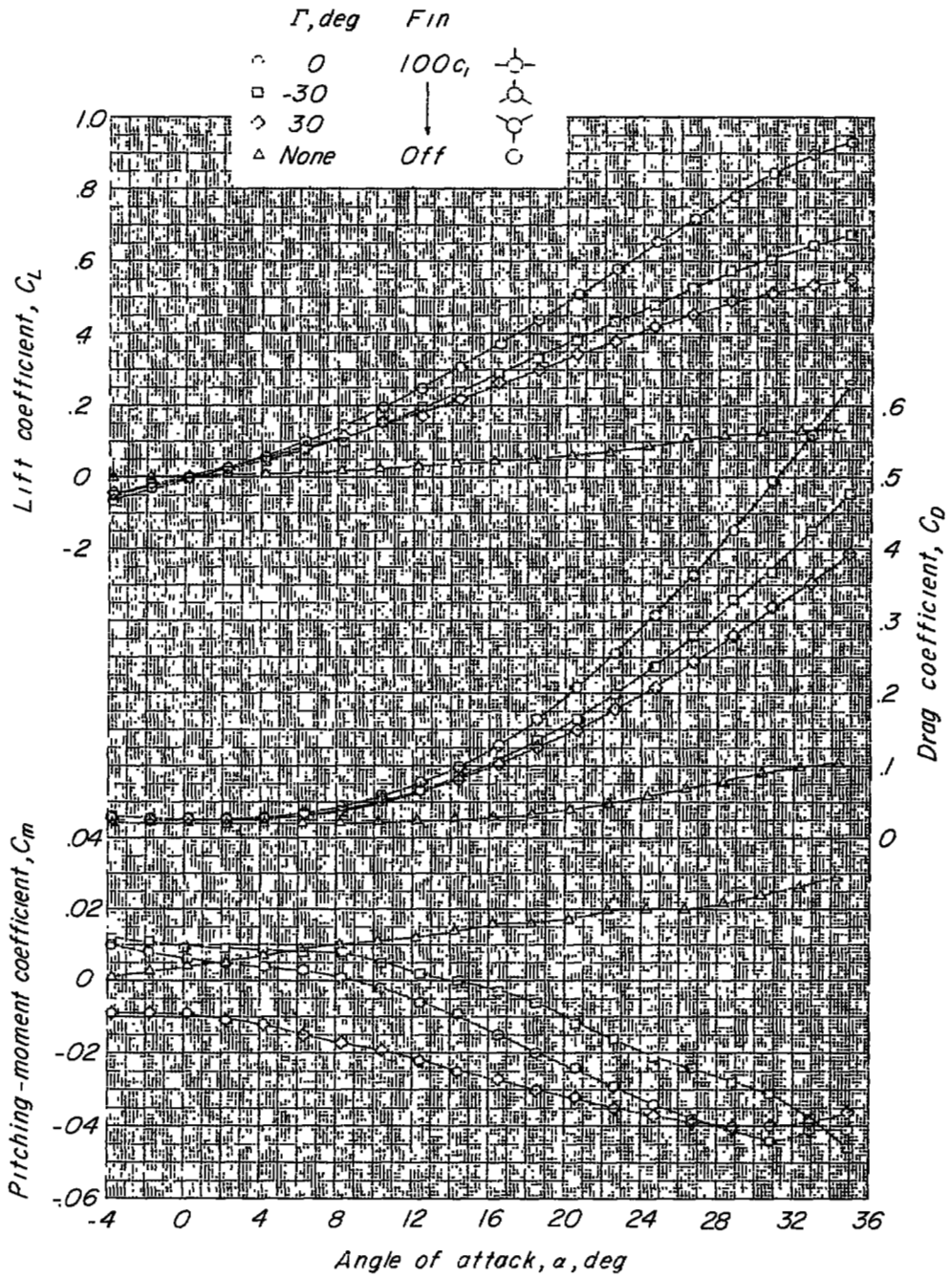

(a) Stability axes.

Figure 3.- Variation of longitudinal coefficients in pitch of the various wing-fuselage combinations and fuselage alone about the stability and body axes. q = 60.

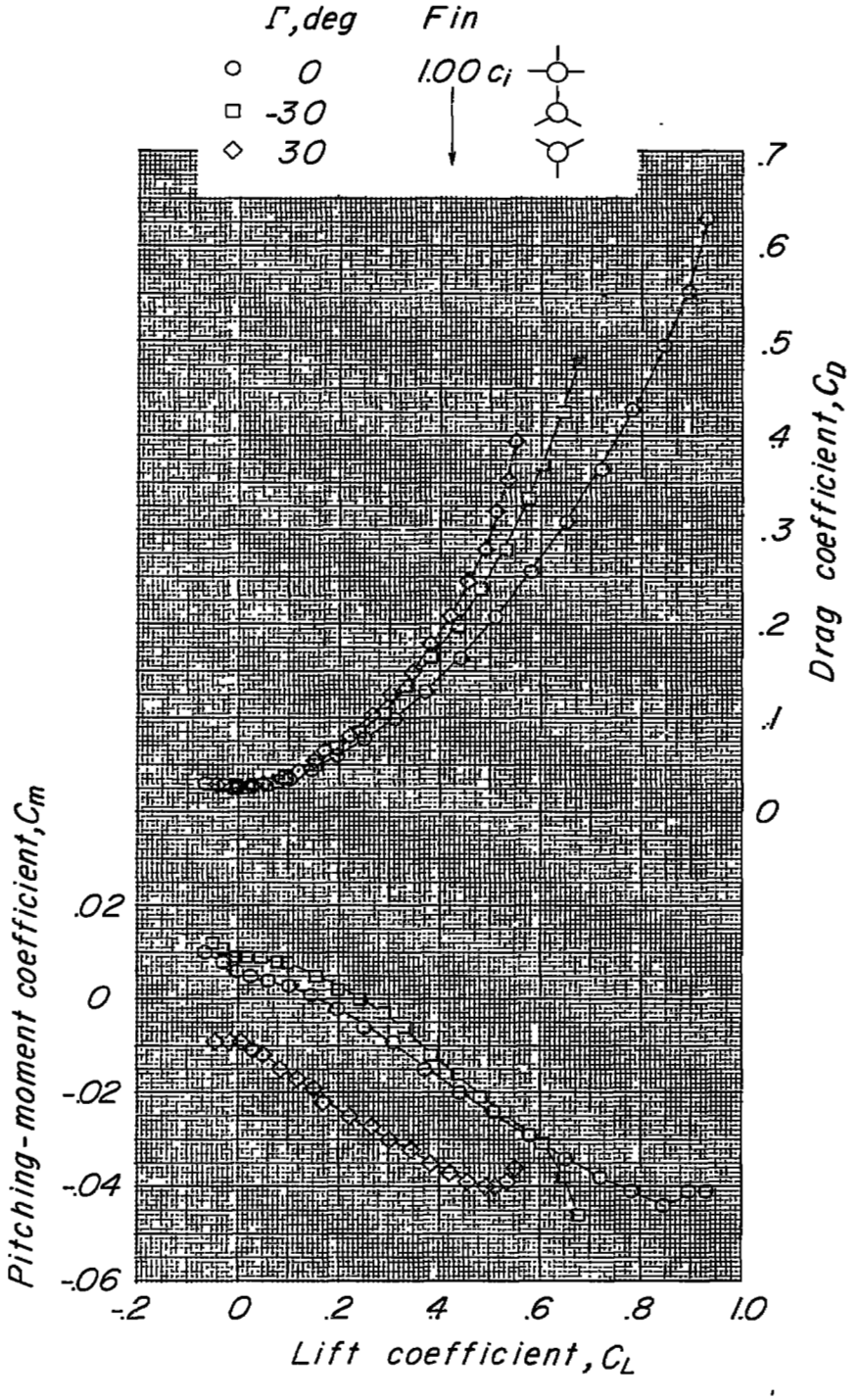

(a) Concluded.

Figure 3.- Continued.

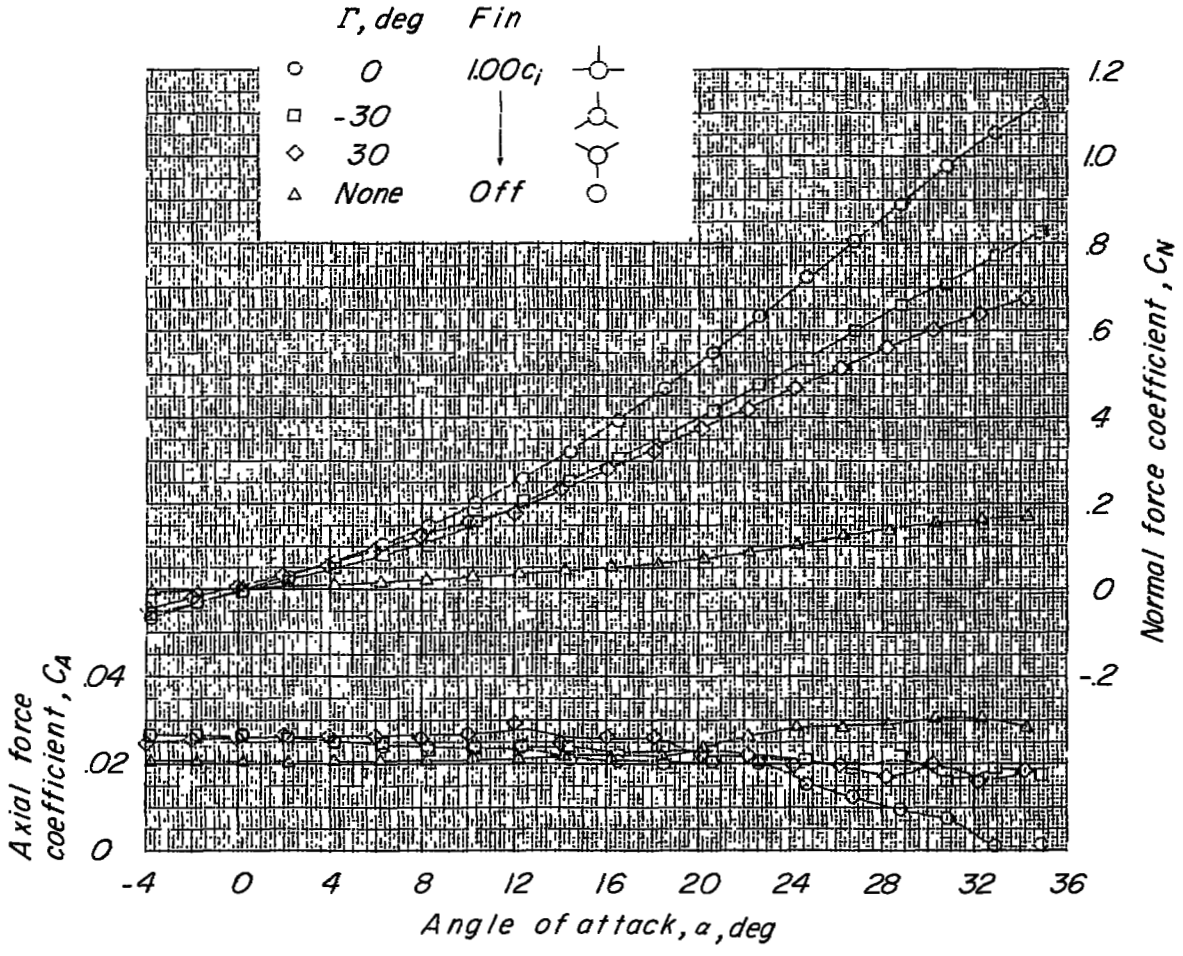

(b) Body axes.

Figure 3.- Concluded.

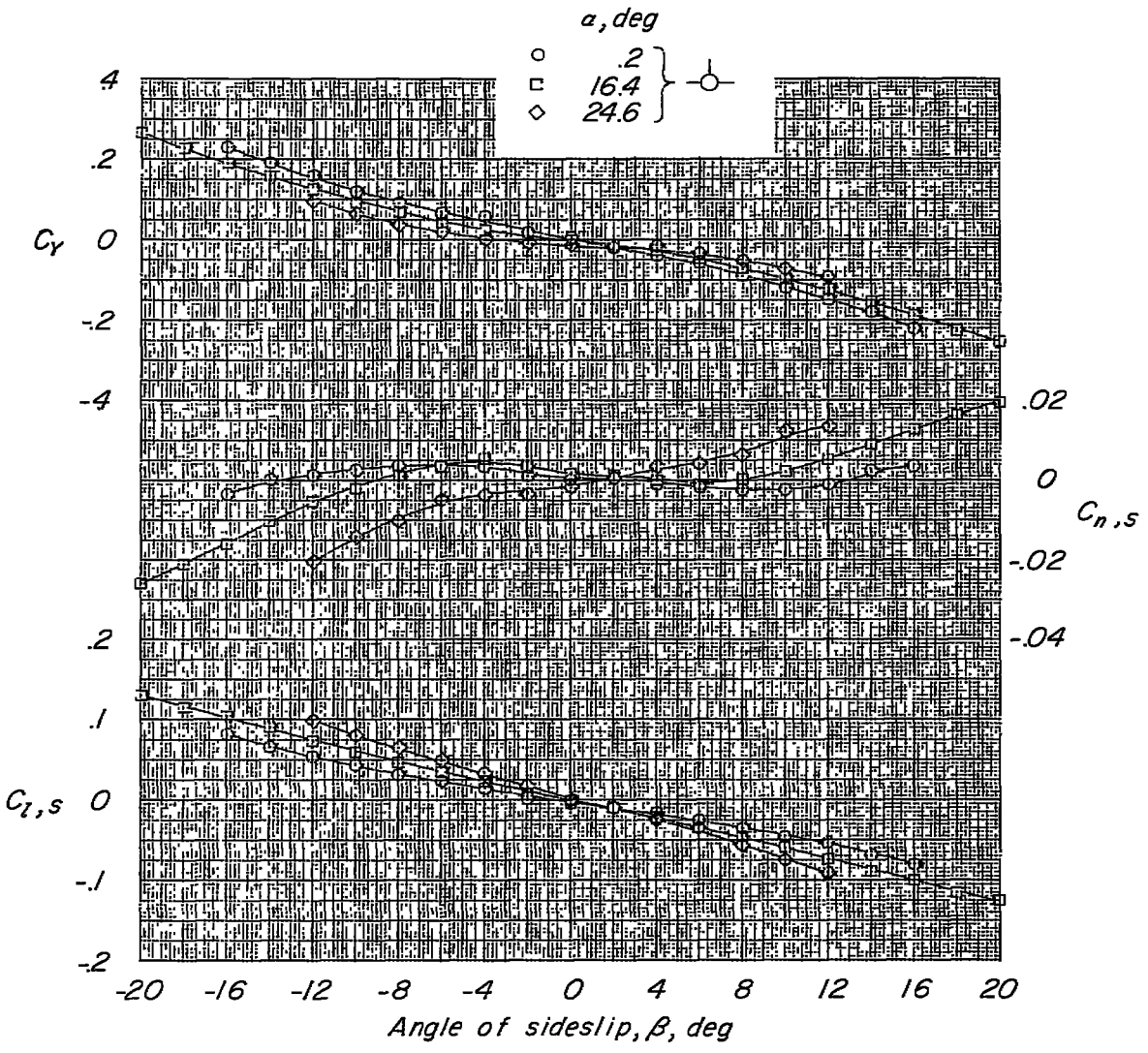

(a) Stability axes.

Figure 4.- Variation of lateral coefficients with angle of sideslip for model with $\Gamma = 0^\circ$ and $1.00c_1$; fin about the stability and body axes. $q = 40$.

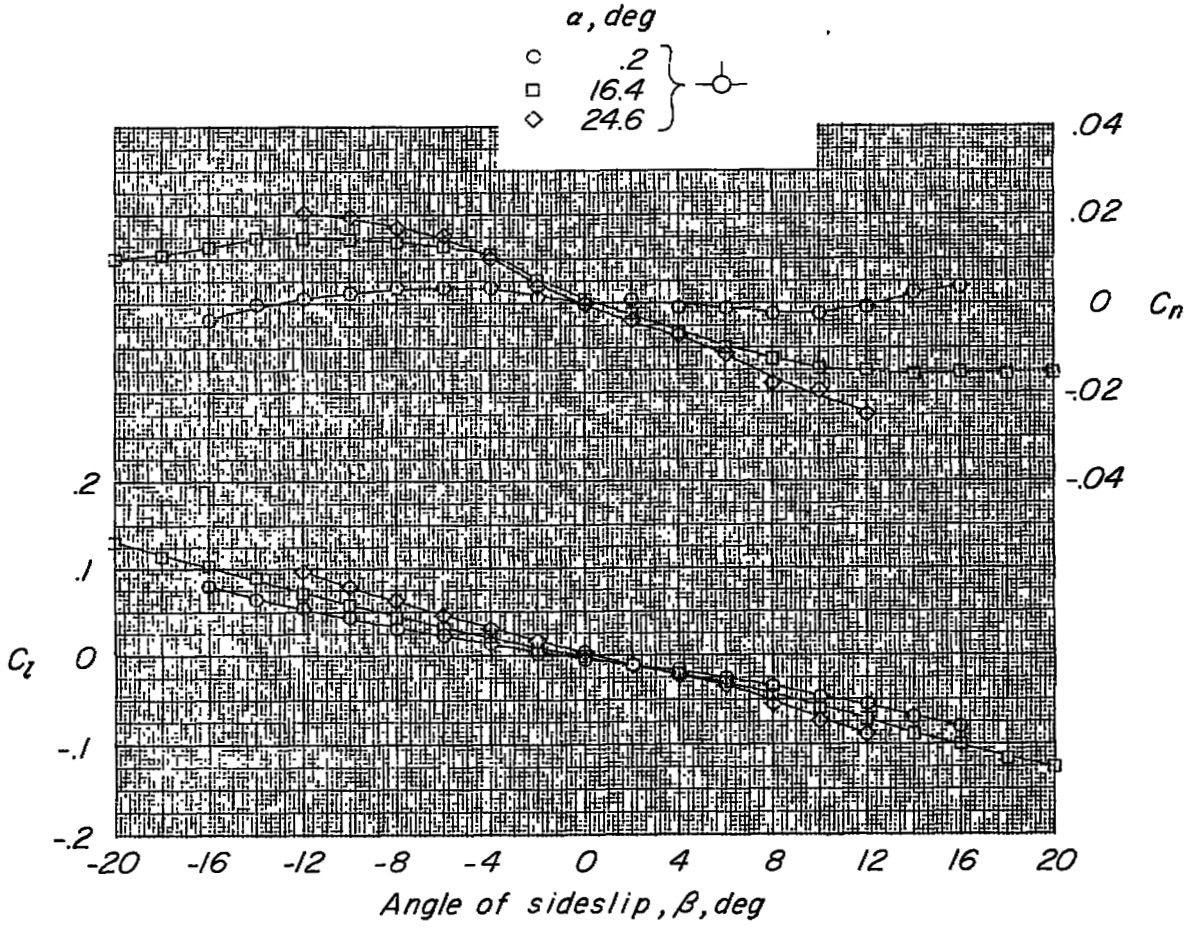

(b) Body axes.

Figure 4.- Concluded.

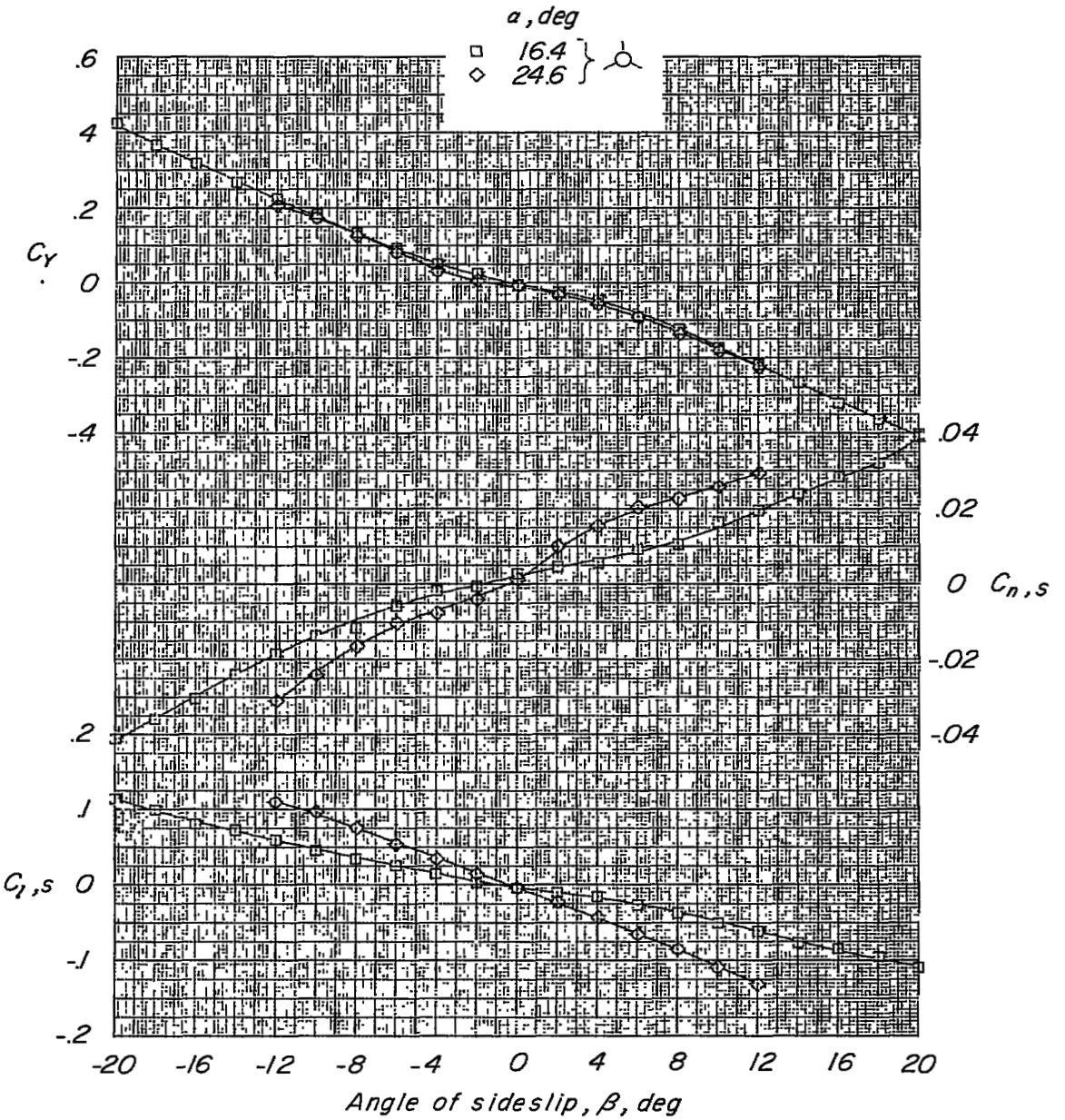

(a) Stability axes.

Figure 5.- Variation of lateral coefficients with angle of sideslip for model with $\Gamma = -30^\circ$ and $1.00c_i$; fin about the stability and body axes. $q = 40$.

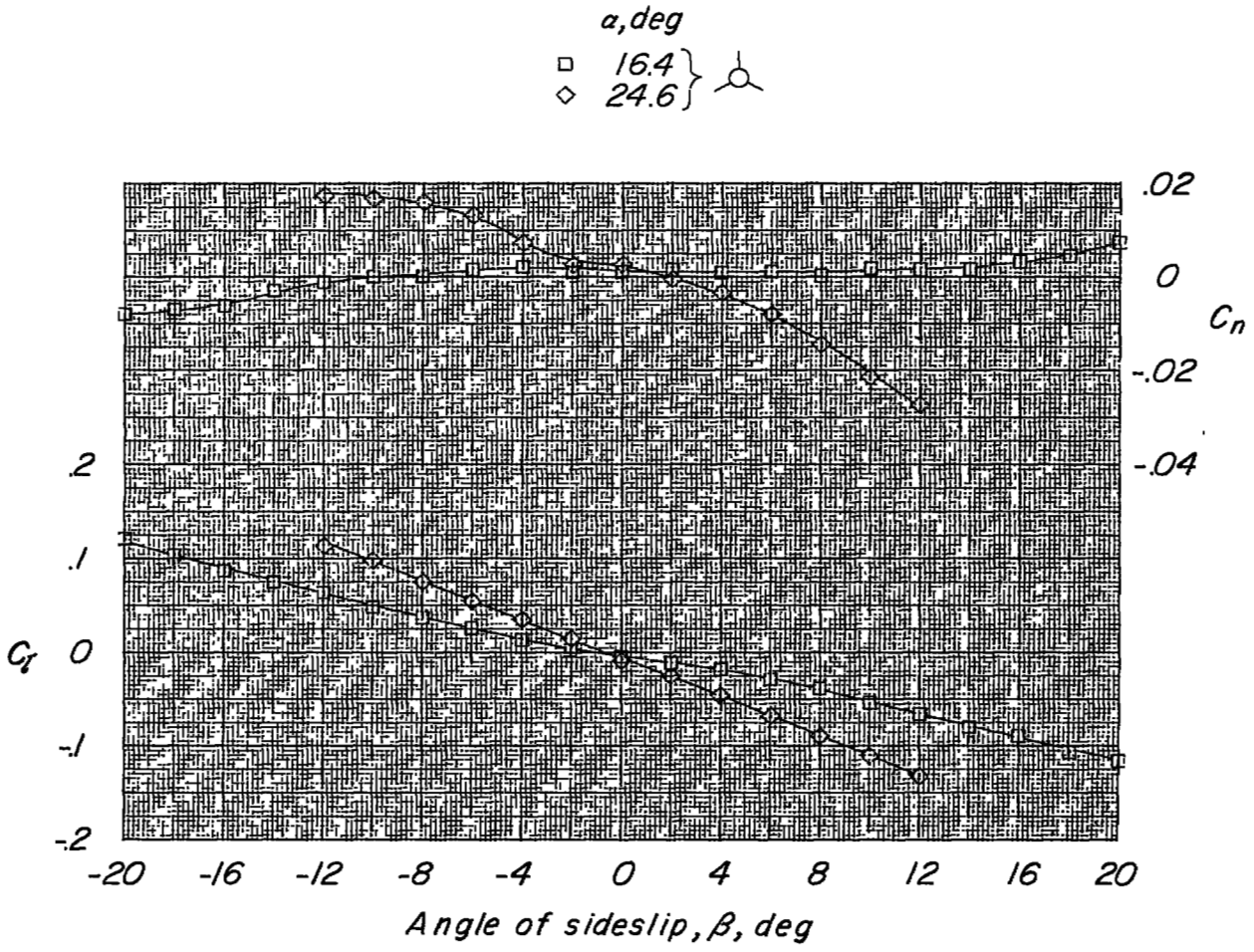

(b) Body axes.

Figure 5.- Concluded.

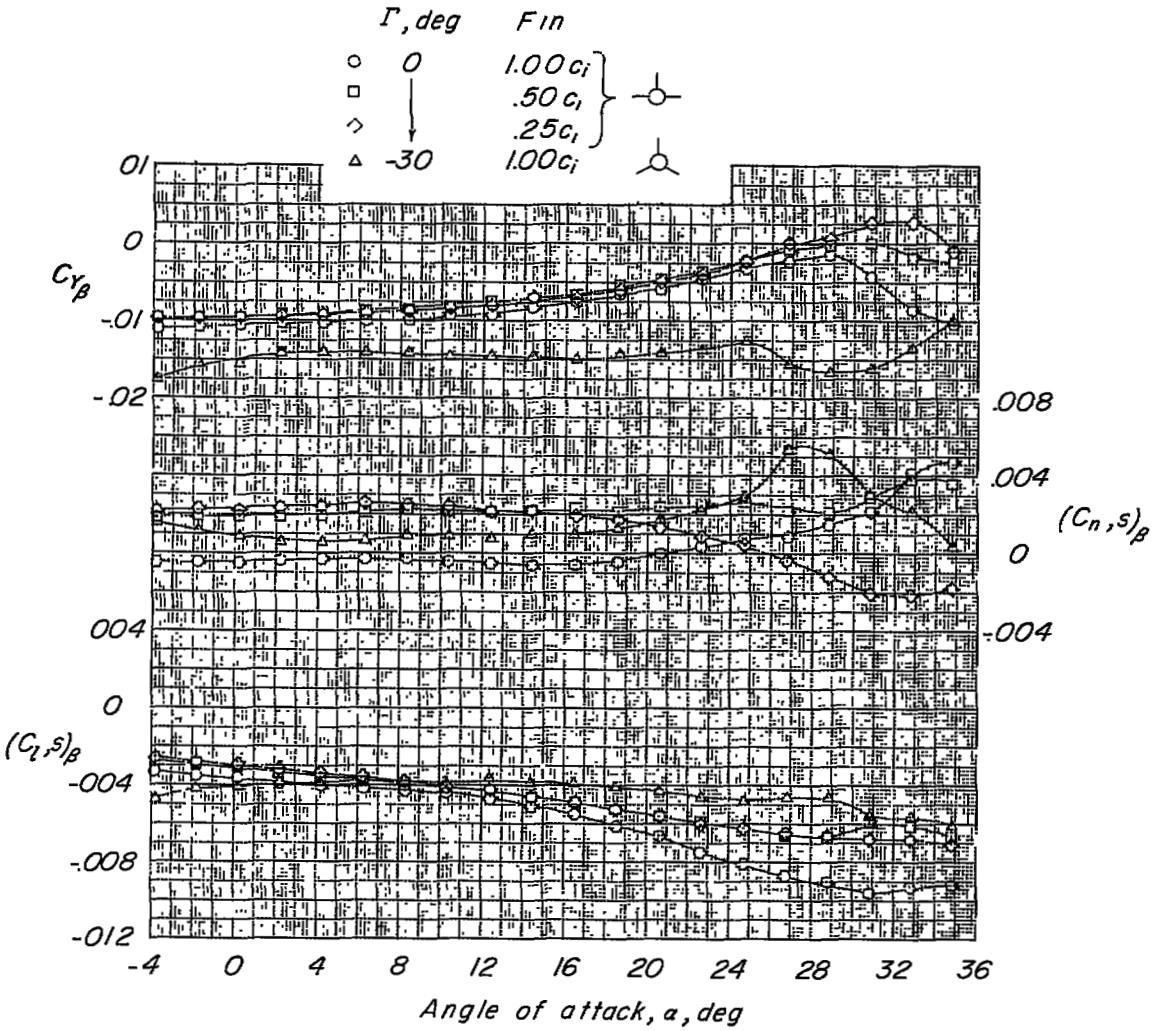

(a) Stability axes.

Figure 6.- Variation of lateral-stability parameters with angle of attack and lift coefficient about the stability and body axes. Effects of negative dihedral and fin size; fins above fuselage; q = 60.

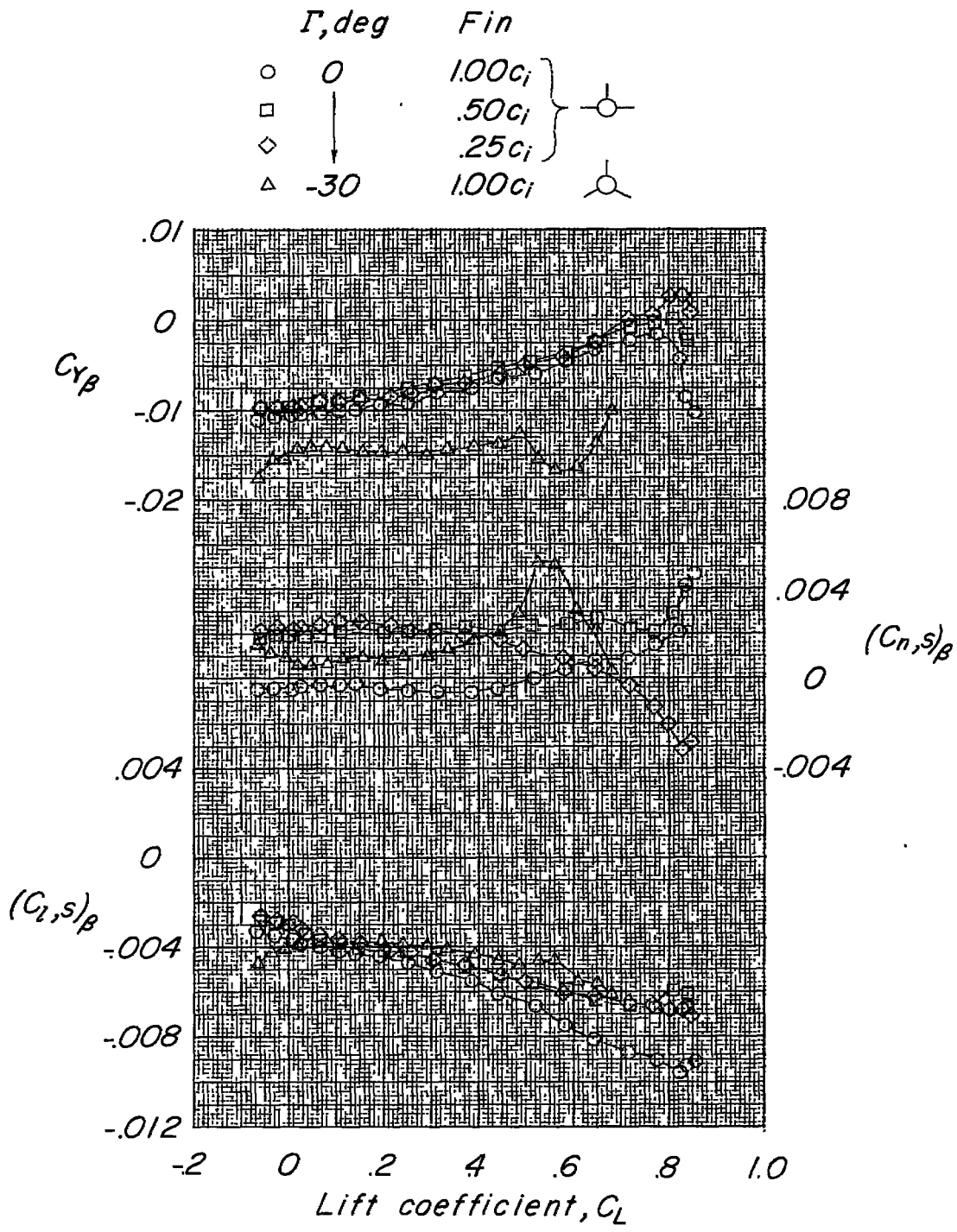

(a) Concluded.

Figure 6.- Continued.

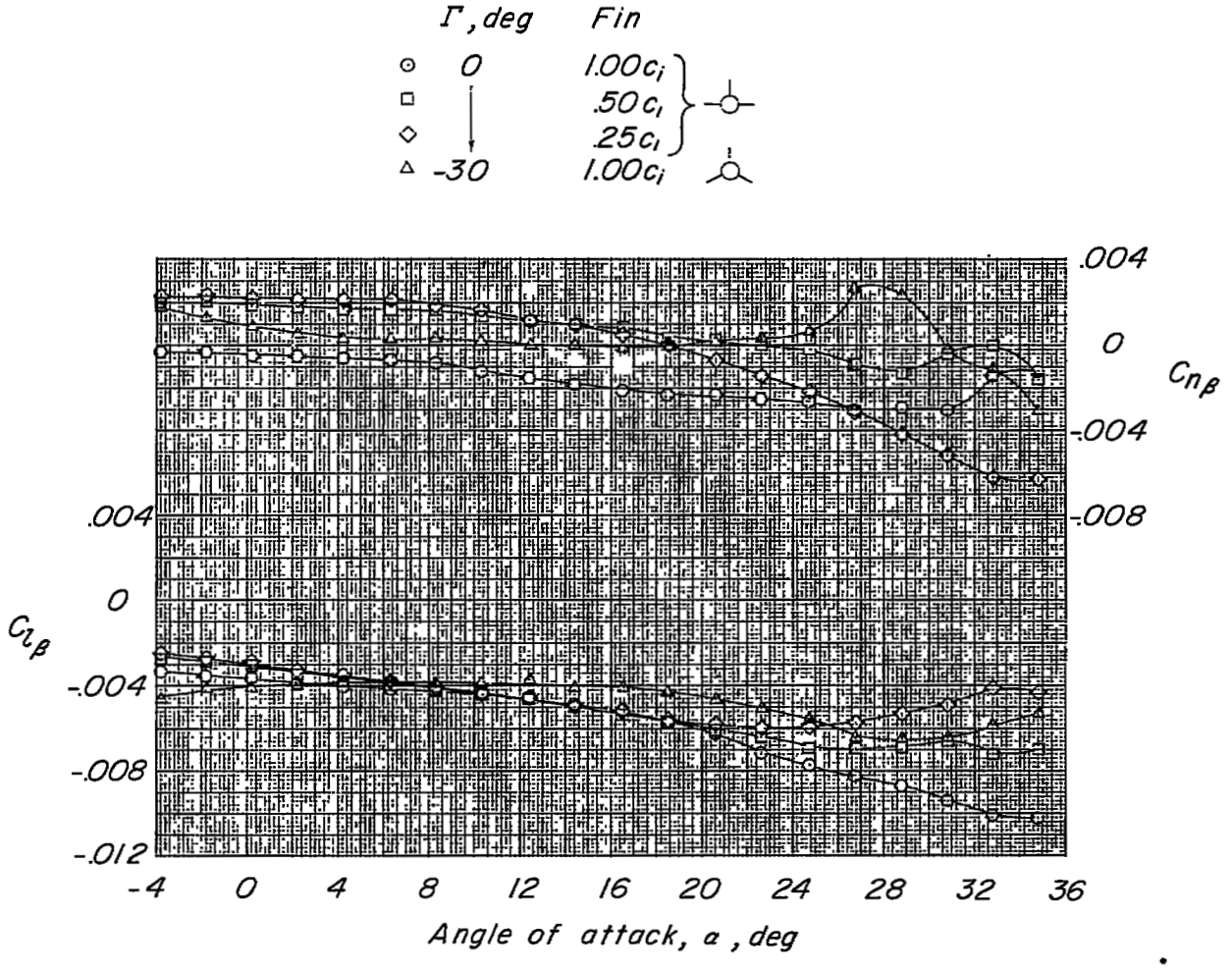

(b) Body axes.

Figure 6.- Continued.

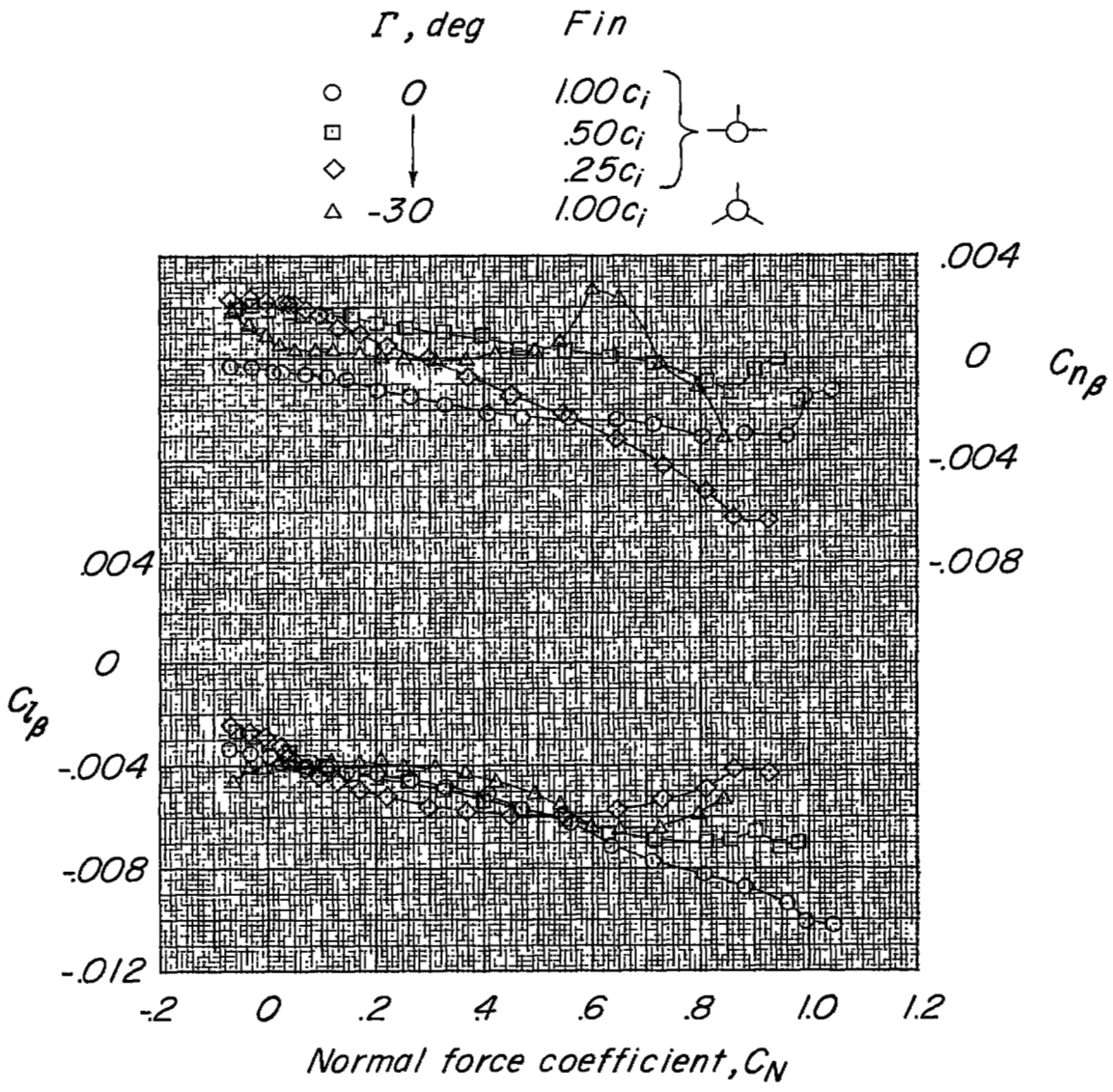

(b) Concluded.

Figure 6.- Concluded.

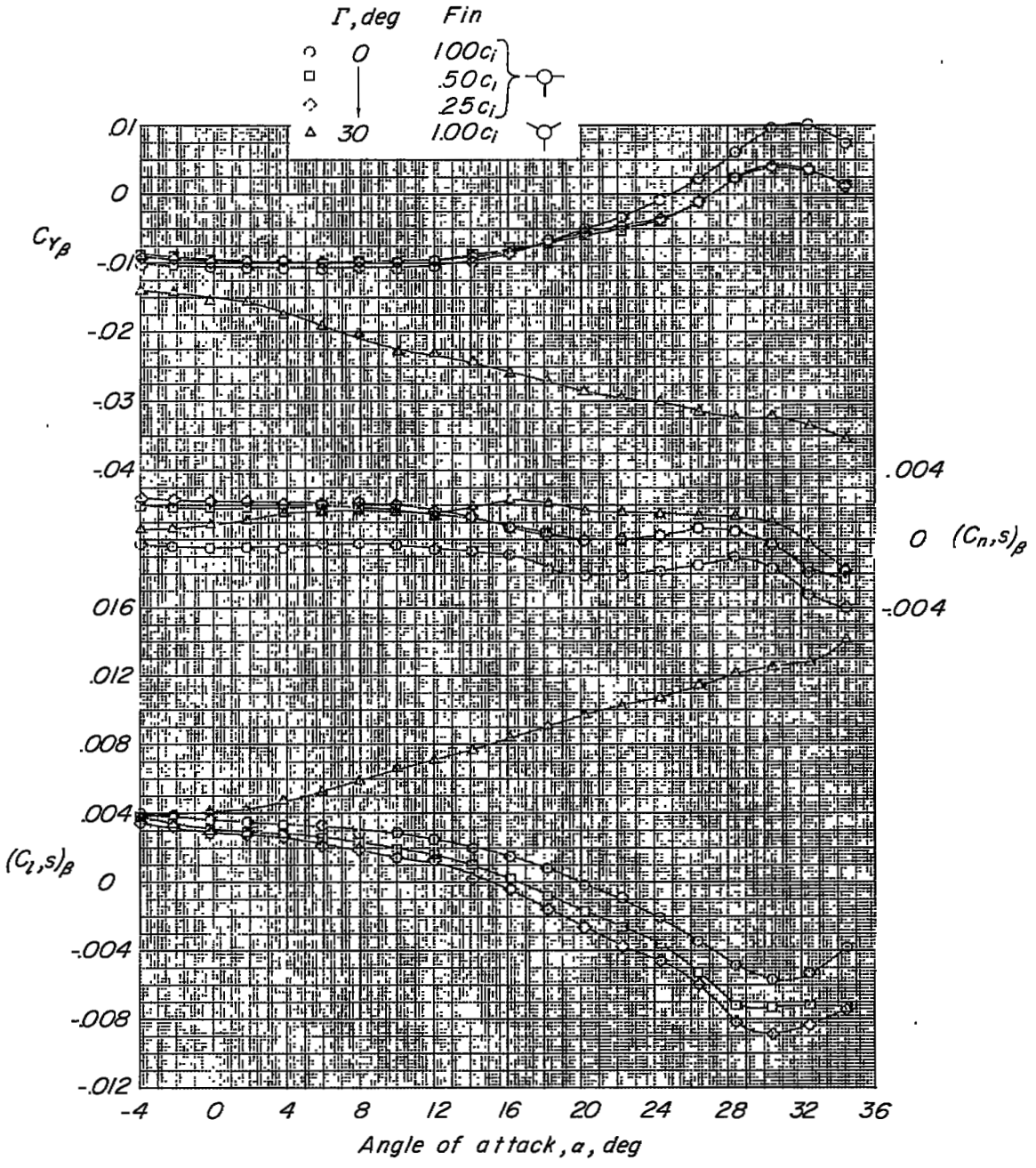

(a) Stability axes.

Figure 7.- Variation of lateral-stability parameters with angle of attack and lift coefficient about the stability and body axes. Effects of dihedral and fin size; fins below fuselage; q = 60.

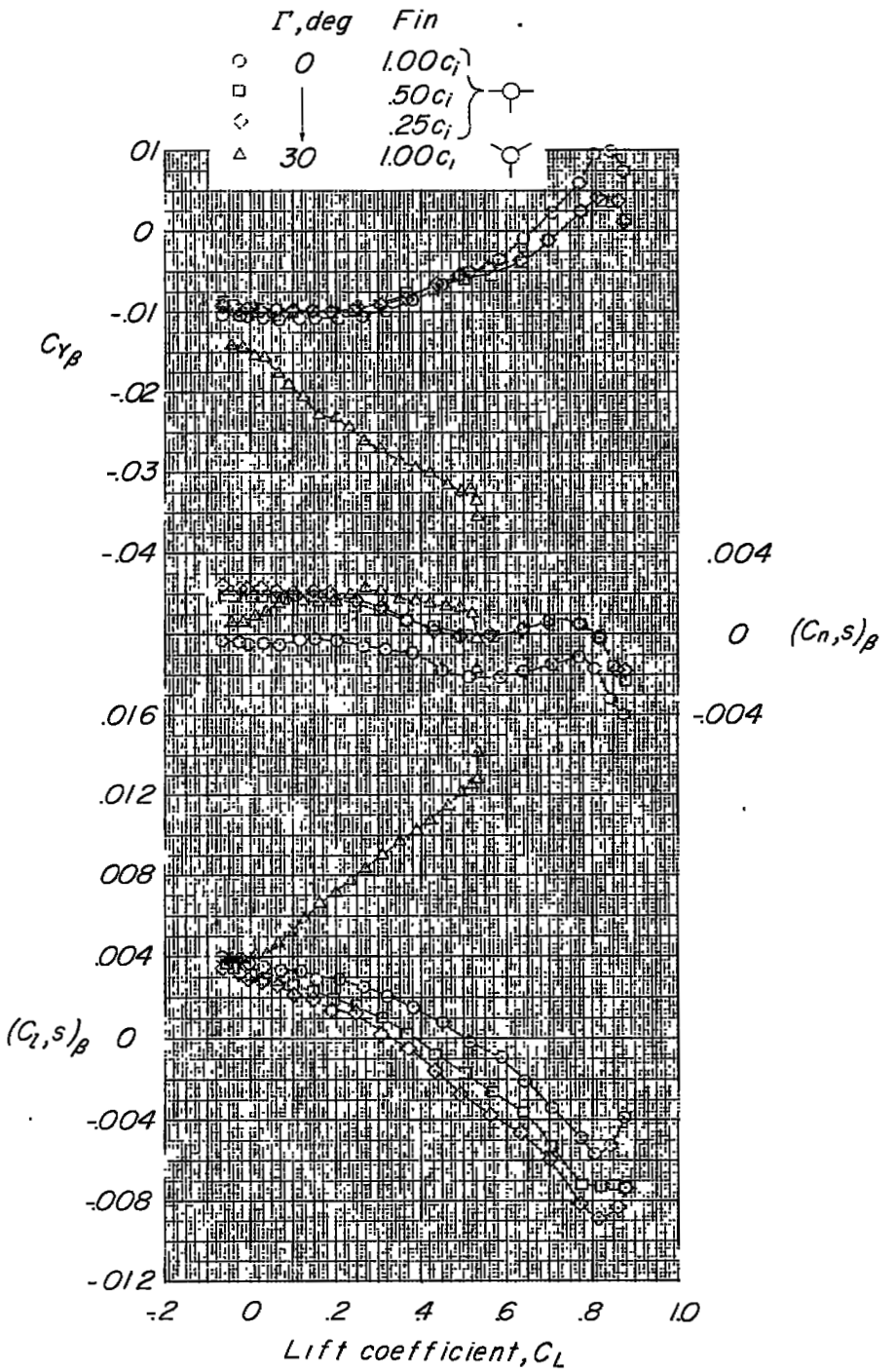

(a) Concluded.

Figure 7.- Continued.

[redacted]

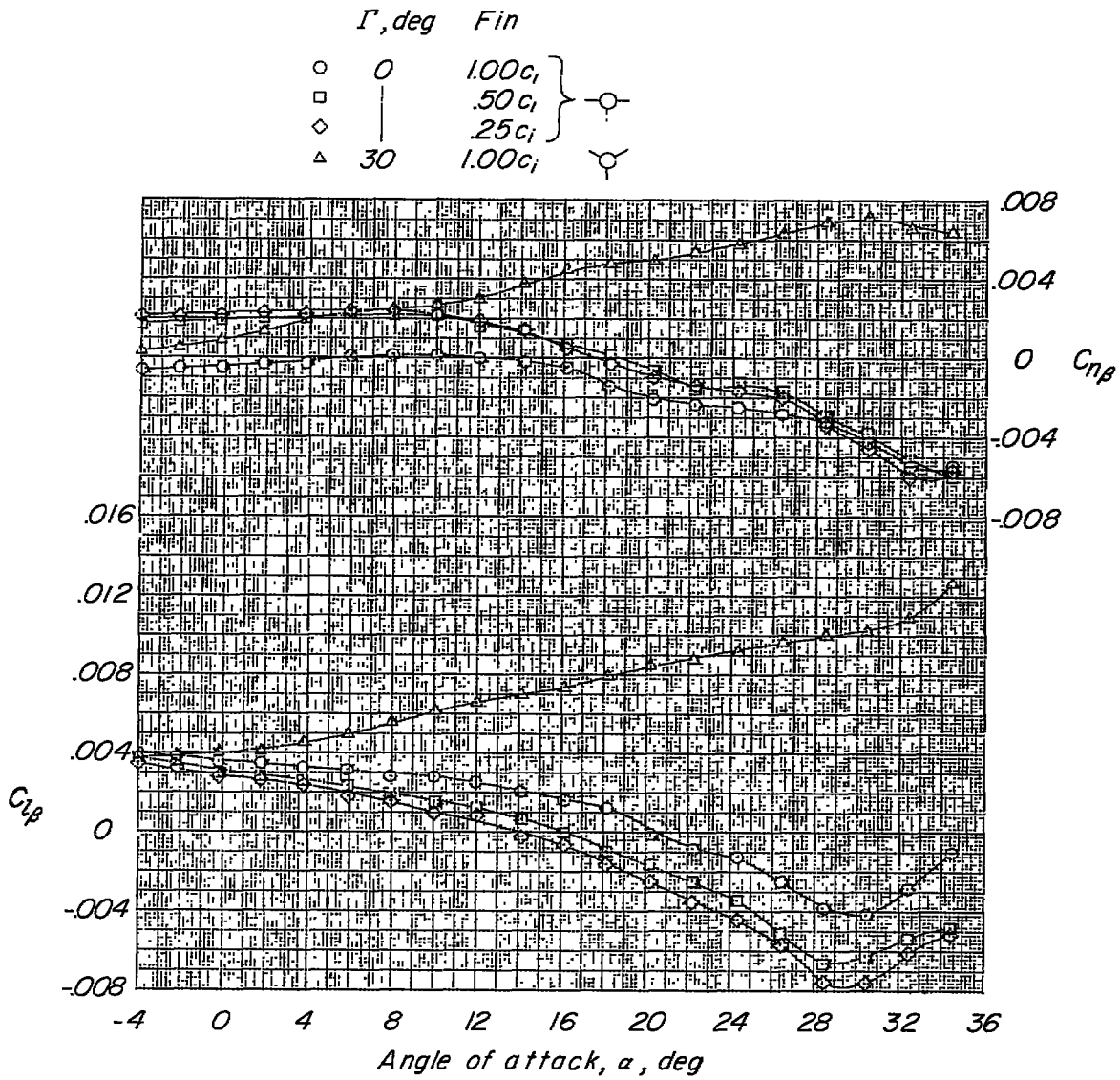

(b) Body axes.

Figure 7.- Continued.

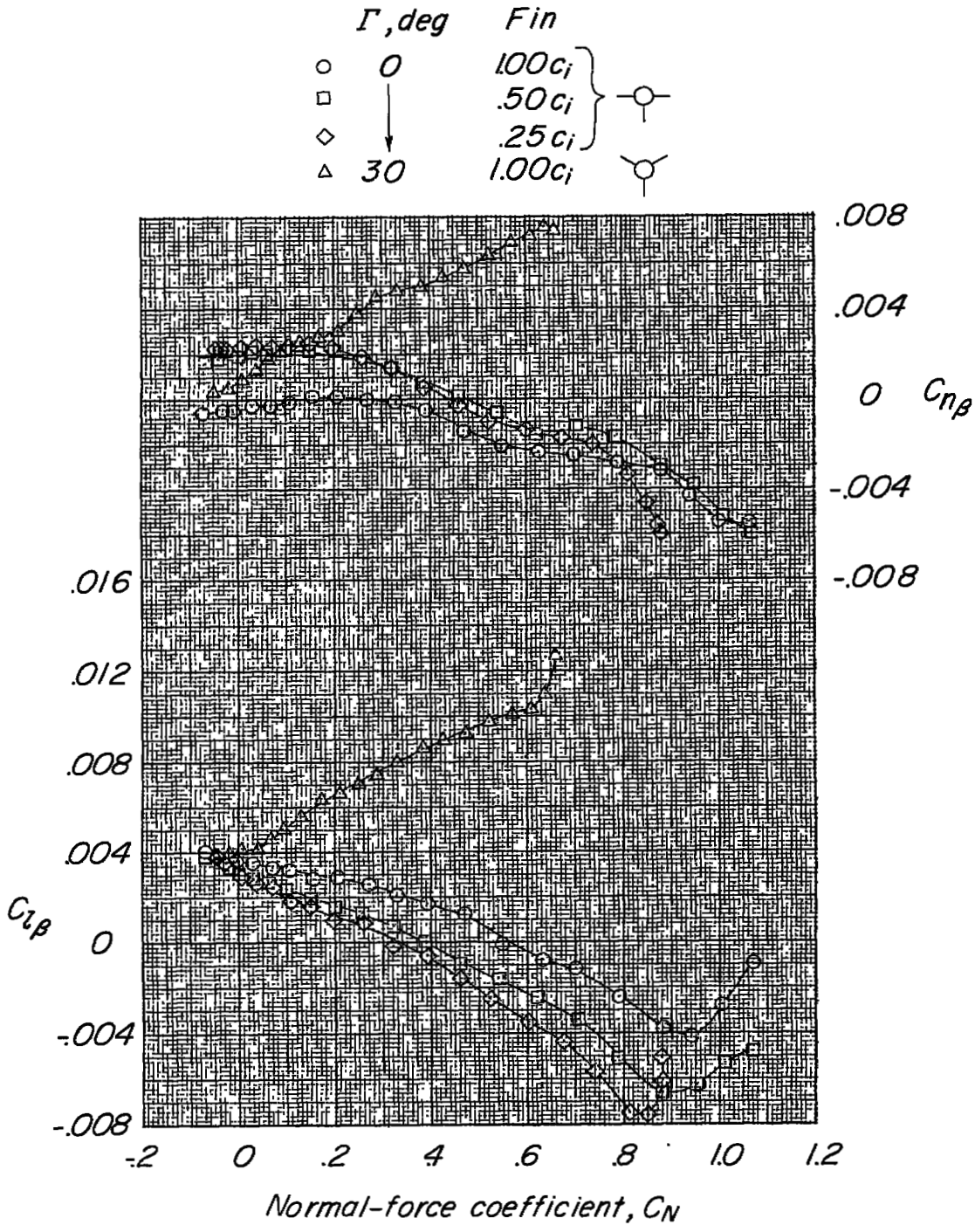

(b) Concluded.

Figure 7.- Concluded.

[redacted]

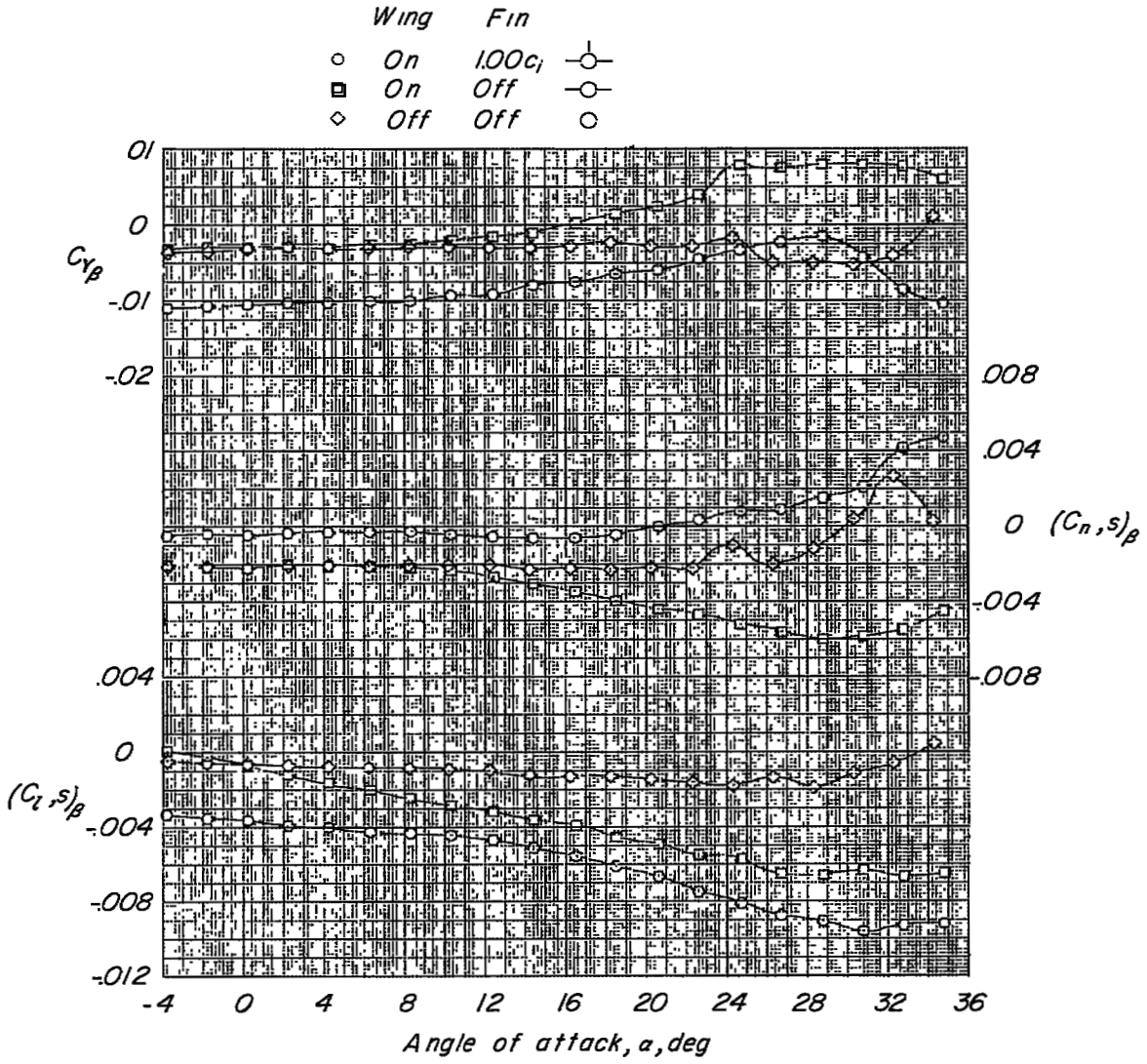

(a) Stability axes.

Figure 8.- Variation of lateral-stability parameters with angle of attack and lift coefficient about the stability and body axes. Effects of removing fins and wing; q = 60.

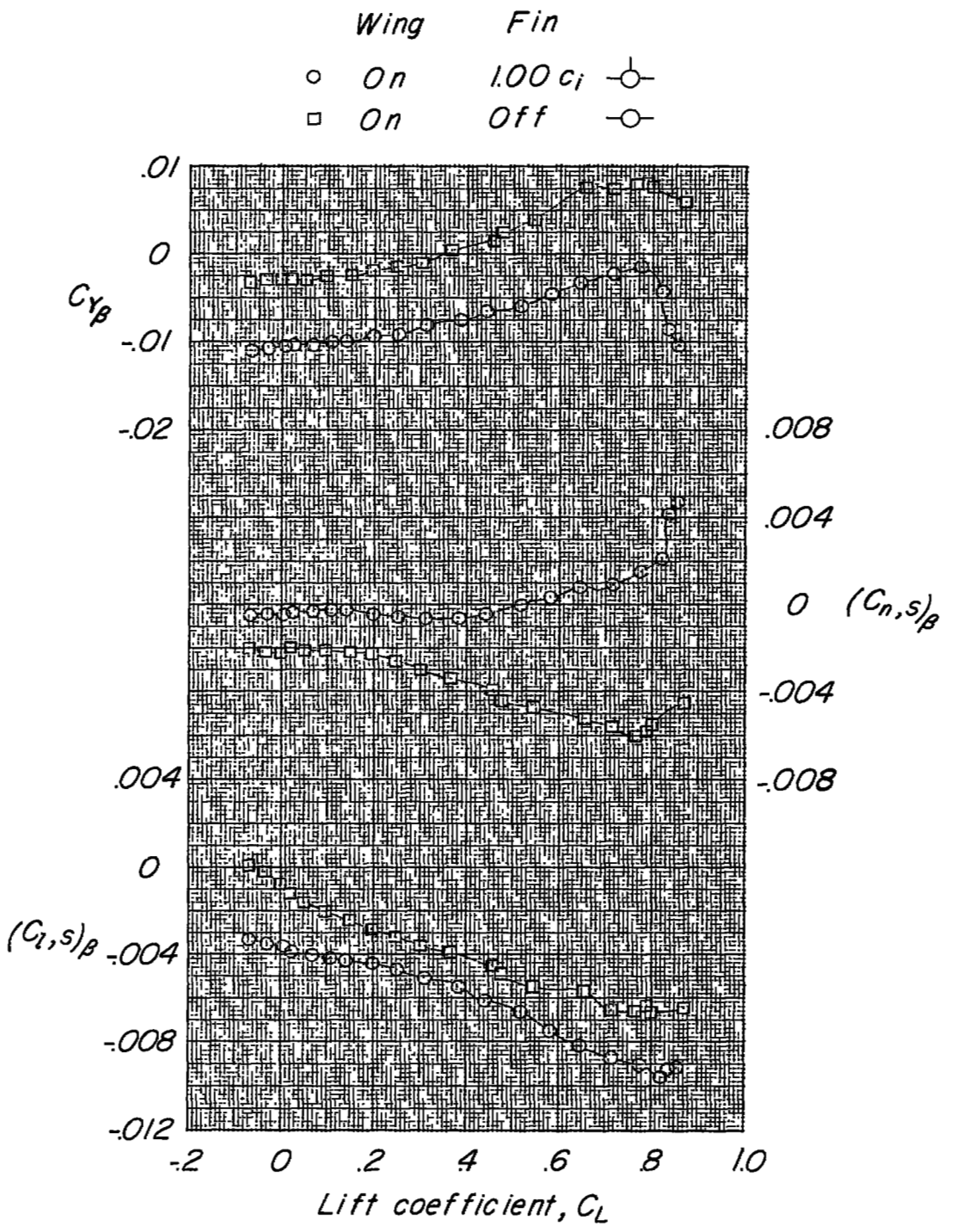

(a) Concluded.

Figure 8.- Continued.

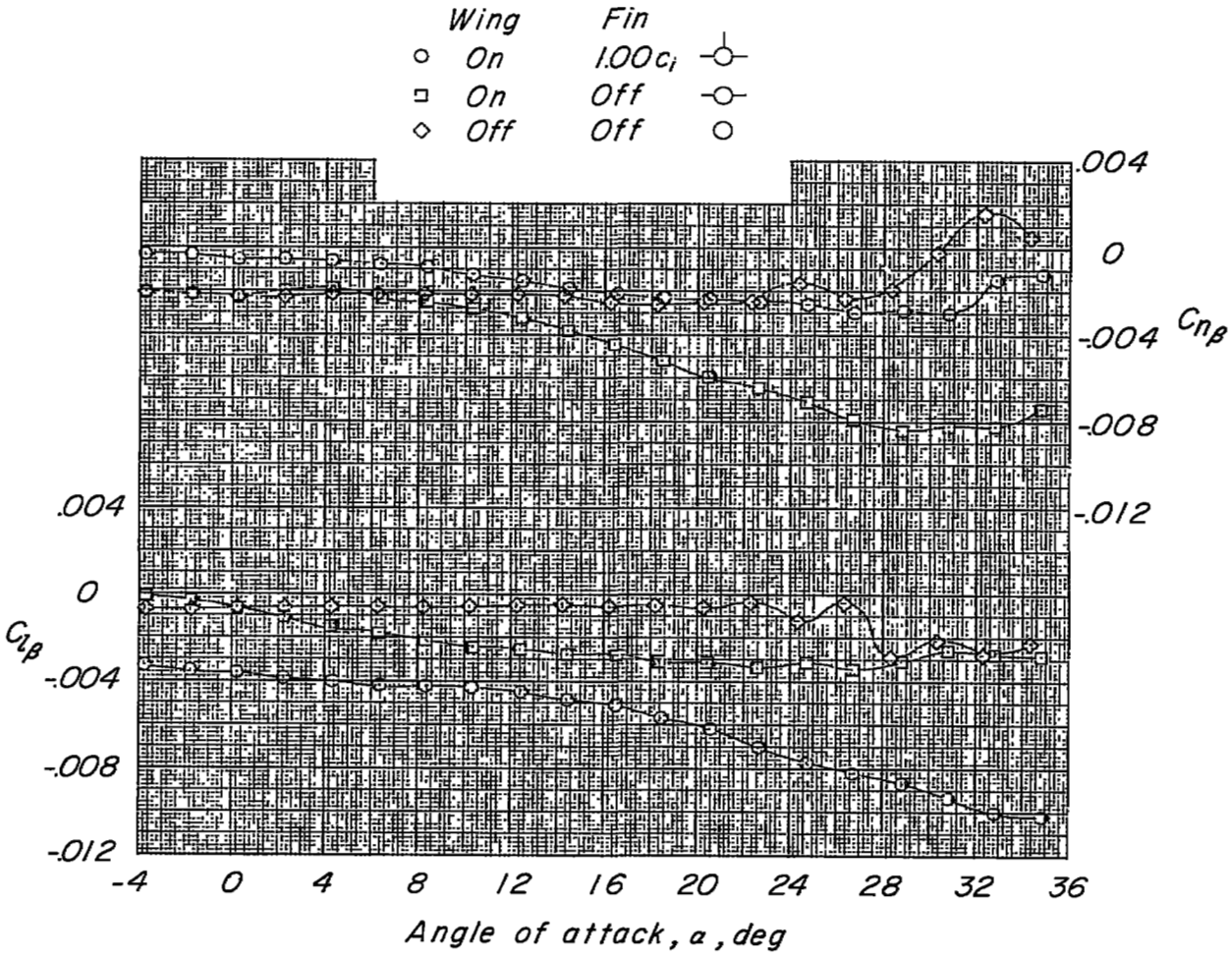

(b) Body axes.

Figure 8.- Continued.

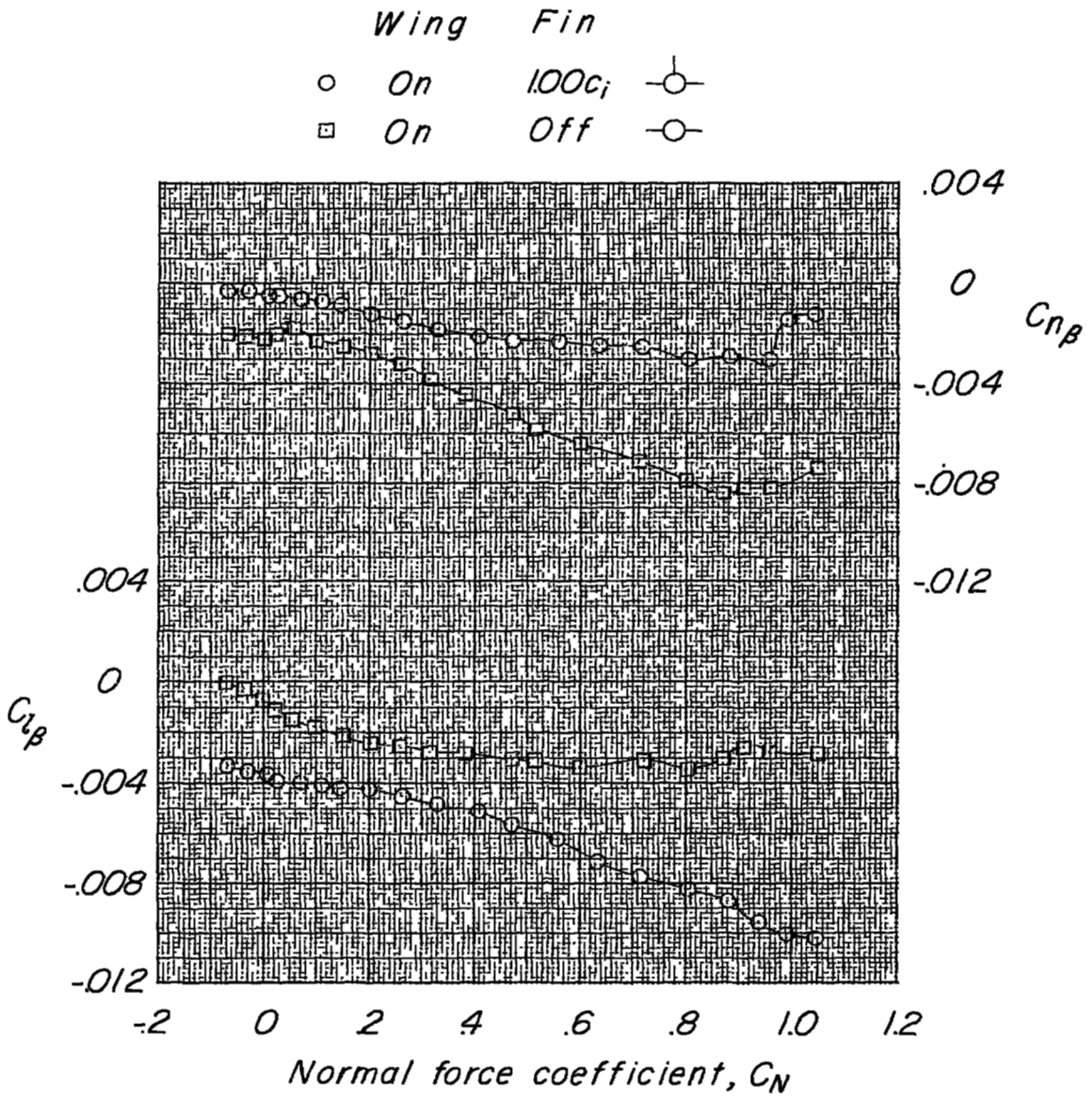

(b) Concluded.

Figure 8.- Concluded.

NACA - Langley Field, Va.